

APPENDIX B: ANALYSES WITH NO CULVERT

1. Introduction

In an effort to determine the effects of the large culvert located near the base of the monolith, a series of analyses was performed for a solid monolith in which the culvert was not considered. Analysis procedures were identical to those described in Appendix A. The open area of the culvert was eliminated by simply adding elements and nodes to the mesh shown in Figure A-4 of Appendix A. Material properties and applied loads for this investigation were identical to those used for the analyses in which the culvert was considered.

2. Analysis and Results

a. Estimation of crack length.

(1) A series of nine analyses, each with a different specified crack length, was performed to compute an initial estimate of the final crack length. The prescribed crack lengths for these analyses ranged from 6.0 ft to 18.0 ft in 1.5-ft increments. No analyses were performed for crack lengths greater than 18.0 ft because the value of K_I for $a = 18$ ft was negative and K_I was positive for all prior analyses. The final crack length of 16.65 ft was found by re-meshing and comparing K_I to K_{Ic} as described in paragraph 3d(1) of Appendix A. The results of each analysis are summarized in Table B-1. The variations of K_I and K_{II} over the range of crack lengths are shown in Figure B-1.

(2) The final crack length computed using the traditional method of analysis was 19.62 ft. The fracture mechanics based prediction of 16.65 ft is only 15.1% less than the value of 19.62 ft computed using the traditional analysis method. When the culvert was considered, the discrepancy between the final crack lengths was 43.7% (see Appendix A), which is slightly more than three times the 15.1% of this case. The fact that the estimated crack lengths are in much better agreement when the culvert is not considered indicates that the rigid behavior assumed by the traditional method of analysis more closely approximates the actual behavior as the monolith becomes stiffer. This should be expected since a solid monolith would behave more like a rigid block than one with a large culvert. Based on this observation, the assumption of a rigid monolith in the traditional method of analysis does not appear to be valid when a large culvert is present.

b. Normal stress profiles.

(1) The normal stress profile along the base of the monolith for a crack length of 16.65 ft is shown in Figure B-2. In order to contrast the difference between the traditional and proposed methods of analysis, the normal stress profile from the traditional method of analysis is also included in Figure B-2. The distance along the base of the monolith is measured from the toe of the monolith to the heel of the monolith and a negative stress indicates compression. Comparison of the normal

Table B-1
Summary of Finite Element Analyses With No Culvert

a ft	K_I ksi $\sqrt{\text{in.}}$	K_{II} ksi $\sqrt{\text{in.}}$	CMOD in.	ΔH_{crest} in.
6.00	0.566	0.628	0.00715	-0.0667
7.50	0.500	0.648	0.00791	-0.0690
9.00	0.435	0.665	0.00859	-0.0712
10.50	0.366	0.682	0.00919	-0.0732
12.00	0.291	0.700	0.00969	-0.0750
13.50	0.209	0.719	0.01006	-0.0764
15.00	0.117	0.740	0.01028	-0.0775
16.50	0.012	0.764	0.01028	-0.0780
16.65	0.000	0.766	0.01027	-0.0770
18.00	-0.108	0.792	0.00962	-0.0748

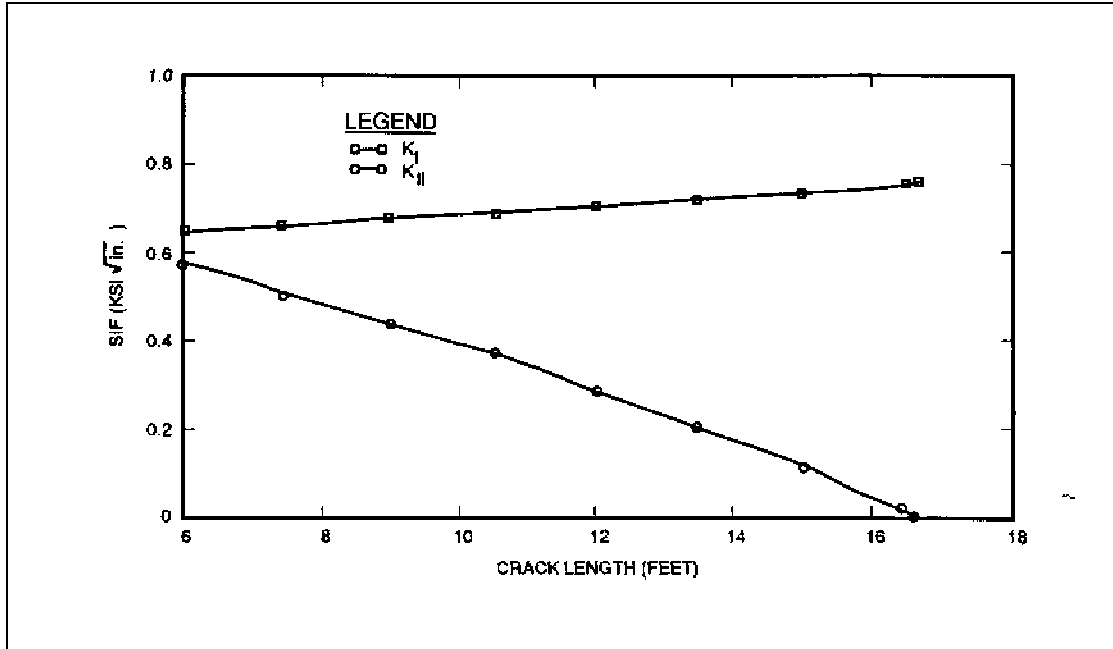


Figure B-1. K_I and K_{II} versus crack length for monolith: no culvert

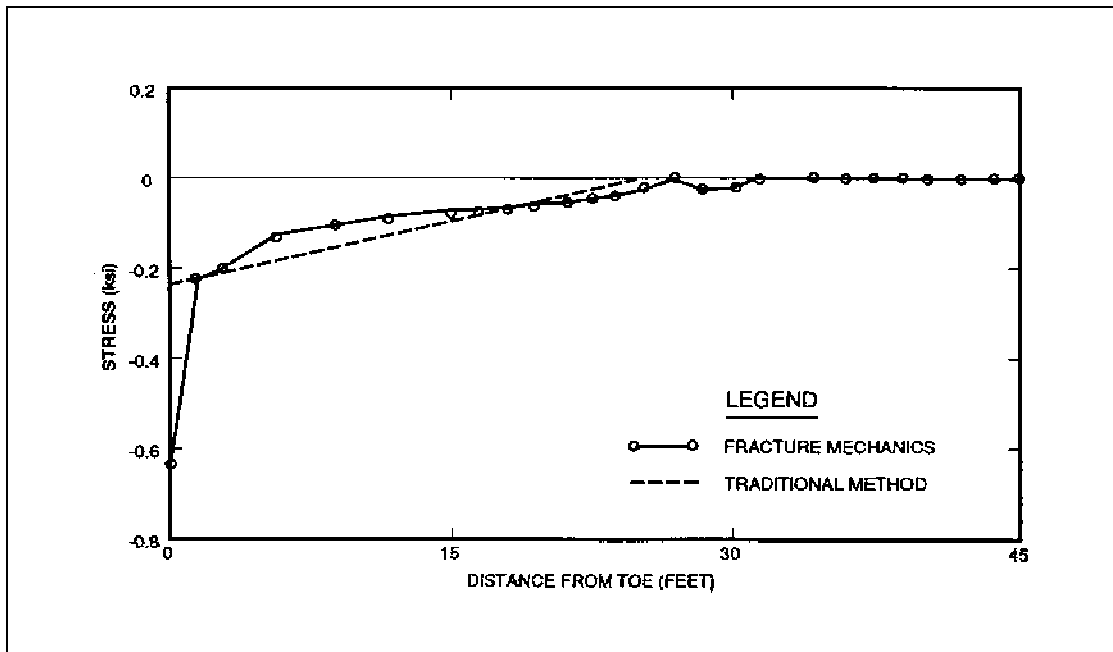


Figure B-2. Normal stress profile at the base of monolith for $a = 16.65$ ft: no culvert

stress profiles of the no-culvert case (Figure B-2) and the actual case (Figure A-11 of Appendix A) shows the effect of the culvert on the normal stress profile. The variation of normal stresses to near zero values between 15.0 and 25.0 ft in Figure A-11 of Appendix A does not exist in the stress profile of Figure B-2. The normal stress profile of Figure B-2 exhibits a near linear response from a location near the monolith toe to the crack tip. This response is more closely approximated using the traditional method of analysis. This provides further validity to the argument that the proximity of the culvert to the base of the monolith has a substantial effect on the transfer of normal stresses in that region.

(2) The resultant force in the vertical direction and the line of action for the resultant force were computed for the finite element solution (as described in paragraph 3d(4) of Appendix A) and for the traditional analysis technique. An equivalent force system with a crack length of 16.65 ft rather than the final crack length of 19.62 ft was used in the computations using assumptions of the traditional analysis technique. The calculated resultant force for the finite element analysis was 447.97 kips

as opposed to 440.56 kips for the traditional analysis technique. The line of action for the resultant force from the finite element analysis was 8.58 ft to the right of the toe as opposed to 8.57 ft from the traditional analysis technique.

c. Shear stress profile. The shear stress profile along the base of the monolith for a crack length of 16.65 ft is shown in Figure B-3. The distance along the base of the monolith is measured from the toe of the monolith to the heel of the monolith. The effect of the culvert is shown further by comparison of results of the no culvert case (Figure B-3) and the case considering the culvert (Figure A-12 of Appendix A). The shear stress profile of Figure B-3 is relatively constant except for the edge effects. However, the variation in shear stresses of Figure A-12 of Appendix A is more significant. The resultant horizontal force was computed for the finite element solution by integration of the stress along the base of the monolith and the traditional analysis technique. The resultant force from the finite element analysis was 247.45 kips as opposed to 249.78 kips from the traditional analysis technique.

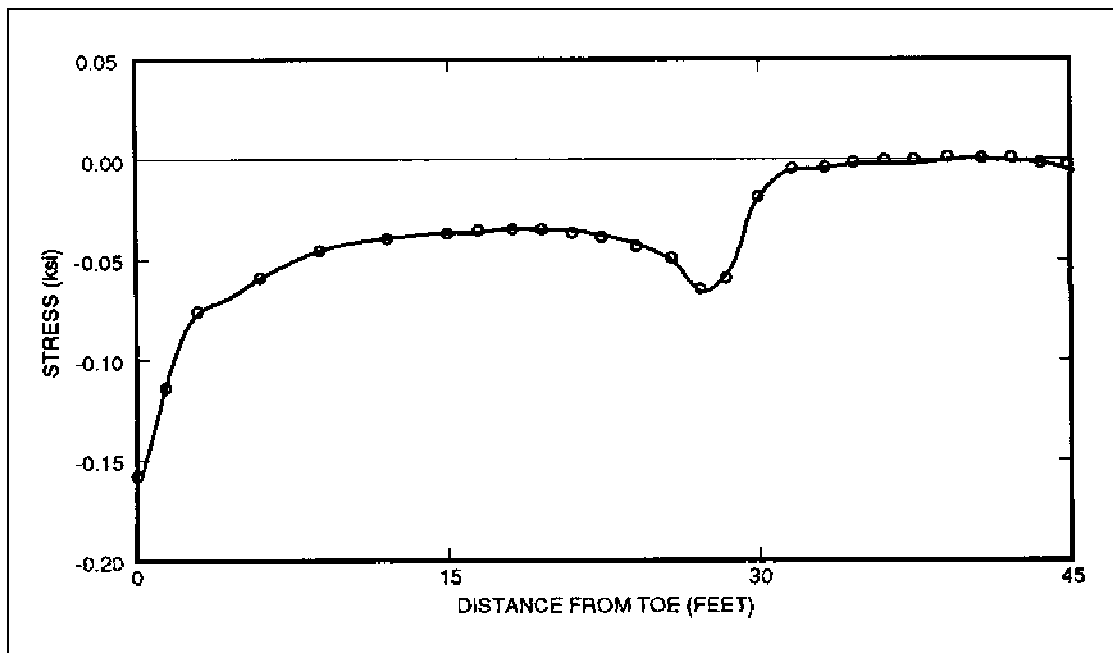


Figure B-3. Shear stress profile at the base of monolith for $a = 16.65$ ft: no culvert